ECOHYDROLOGY
Ecohydrol. **5**, 467–477 (2012)
Published online 7 June 2011 in Wiley Online Library
(wileyonlinelibrary.com) DOI: 10.1002/eco.239

The impact of pine beetle infestation on snow accumulation and melt in the headwaters of the Colorado River

Evan Pugh* and Eric Small
Department of Geological Sciences, University of Colorado, Boulder, CO 80309, USA

ABSTRACT

The mountain pine beetle is killing many trees in Colorado's high-elevation forests. The thinned canopies found in dead tree stands should intercept less snow and transmit more radiation than canopies in living forests, altering snow accumulation and melt processes. We compare snow, forest, and meteorological properties beneath living and pine beetle-killed tree stands. Eight pairs of living and dead tree stands were monitored over two years along the headwaters of the Colorado River. During year one, all eight dead stands were in the red phase of tree death — the trees still retained needles. Snow accumulation was the same under living and red phase stands, but snow melt was more rapid in red phase stands. As a result, the snowpack was depleted one week earlier in the red phase stands. Canopy shortwave transmission was not higher in red phase stands. We hypothesize that the faster melt and earlier depletion in red phase stands was caused by accelerated needle loss which lowers the albedo of the snow surface. By year two, many of the dead trees had progressed to the needle-less grey phase of tree death. Snow accumulation in grey phase stands was 15% higher than in paired living stands. Snow in grey phase stands melted more rapidly than in living stands, likely as a result of increased canopy shortwave transmission. We combine our results with those from previous studies to develop a conceptual model that describes how beetle infestation affects snow accumulation and melt in the different stages of mortality. Copyright © 2011 John Wiley & Sons, Ltd.

KEY WORDS forest snow hydrology; mountain pine beetle; snow accumulation; canopy interception; snowmelt; canopy transmission; tree death

Received 2 May 2011; Accepted 8 May 2011

INTRODUCTION

The high-elevation forests that are a primary source for Colorado's domestic and agricultural water needs are changing rapidly due to an infestation by the mountain pine beetle (MPB; *Dendroctonus ponderosae*) (USFS, 2010). MPB are native to Colorado's high-elevation forests. However, the severity of MPB infestation and resulting tree death has increased dramatically over the past 15 years. In Colorado, over 16 000 km^2 of lodgepole (*Pinus contorta*) and ponderosa pine (*Pinus ponderosa*) forest have been infested by MPB since 1996 (USFS, 2011). It is predicted that the current epidemic will kill most of the pines in these areas. Current widespread MPB outbreaks are not limited to Colorado; they are also impacting forests in much of the Western United States and British Columbia, Canada (Ministry of Forests and Range, 2009). The cause of the current widespread MPB outbreaks across North America is unclear, but likely involves multiple factors that include climate change and past land management (Logan *et al*., 2003; Aukema *et al*., 2008; Macias Fauria *et al*., 2009). This study is not focused on establishing the causes of MPB infestation, but instead on quantifying the impacts of widespread tree death on snow accumulation and melt. Understanding the dynamics of mountain snowpack is critical for effective management of water resources in the Western United States.

The current MPB infestation in Colorado's headwaters is causing rapid changes in forest characteristics that will likely impact hydrologic processes. MPB are very destructive to forest canopies, often killing all of the mature trees within lodgepole pine stands (Schmid and Mata, 1996). Evergreen trees do not retain their needles indefinitely, but seasonally shed older and inner needle whorls. On average, healthy lodgepole pines retain needle cohorts for between 9 and 13 years, depending on forest elevation (Schoettle, 1990, 1994; Vose *et al*., 1994). MPB-infested trees lose their needles and woody biomass more rapidly than healthy trees. The process of MPB-induced tree death creates two distinct classes of dead trees. During the first 2 years following death, a lodgepole pine's needles will change color to red and start falling off (Wulder *et al*., 2006). This stage of tree death is termed the 'red phase'. Generally by the end of the third year after infestation, most of a dead lodgepole pine crown has been denuded of needles (Wulder *et al*., 2006). Trees that have been completely denuded of needles are in what is termed the 'grey phase'.

MPB infestation affects forest characteristics that are known to impact accumulation and ablation of snow, which in turn impact the water balance of entire drainage basins (Bales *et al*., 2006). Forest canopies create sheltered subcanopy environments by attenuating the amount of incident solar radiation transmitted to the

* Correspondence to: Evan Pugh, Department of Geological Sciences, University of Colorado, Boulder, CO 80309, USA.
E-mail: evan.pugh@colorado.edu

ground (Hardy *et al*., 2004; Link *et al*., 2004) and intercepting incoming precipitation (Golding and Swanson, 1978; Kattelmann *et al*., 1983; Musselman *et al*., 2008; Molotch *et al*., 2009; Veatch *et al*., 2009). Large portions of that intercepted precipitation sublimate back to the atmosphere (Pomeroy and Schmidt, 1993; Pomeroy and Gray, 1995; Hedstrom and Pomeroy, 1998). Relative to clearings, forests also experience reduced variability in subcanopy humidity and temperature through slower wind speeds (Bernier, 1990), vegetation heat storage, and canopy longwave emission (Raynor, 1971; Rouse, 1984; Link and Marks, 1999; Pomeroy *et al*., 2009). Lower wind speeds and attenuated incoming shortwave radiation lead to slower snowpack ablation (Molotch *et al*., 2009). In snow-dominated regions, forest cover is the strongest predictor of both snow accumulation and ablation (Varhola *et al*., 2010).

To date, studies of the hydrological impacts of MPB infestation have largely been focussed on the water yield from the basin. The effects on snow accumulation and melt have largely been ignored, with the exception of two studies completed in British Columbia (Boon, 2007, 2009). Long-term water yield studies have shown increased runoff from MPB-infested basins that rises to a maximum 15 years after the initial insect infestation (Love, 1955; Hibbert, 1965; Bethlahmy 1974, 1975; Potts, 1984). Changes are still measurable in impacted basins 25 years after the outbreak. These types of studies do not provide a mechanistic understanding of how MPB infestations impact the hydrologic cycle. For example, the contributions from modified snow accumulation and melt processes are not isolated from other effects such as changes in evapotranspiration. Here, we measure how MPB infestation impacts the dynamics of snow accumulation and melt. In addition, we examine the differences in shortwave transmission and surface albedo between the three tree mortality phases to better understand the observed changes in snow dynamics.

The previous studies of the effects of MPB infestation on snow water equivalent (SWE) were completed using data from forests in British Columbia (Boon, 2007, 2009). In both studies, the author measured snow accumulation and ablation in a living stand, a dead stand, and a clearcut. In Boon (2007), 70% of the dead trees were transitioning from the red phase to the grey phase of tree death. The remaining 30% were in the grey phase. In the second study (Boon, 2009), trees in the dead stand were all in the grey phase of death. Boon (2007, 2009) observed more accumulation in the dead stand than in the living stand. This was interpreted to be the result of reduced canopy interception of snow and subsequent sublimation. In the second study, Boon (2009) observed accelerated dead stand ablation. This was caused by increased shortwave radiation resulting from the thinning of the forest canopy. The enhanced accumulation outweighed the faster melting, so the net effect was prolonged snow cover duration under the dead stand.

Boon's (2007, 2009) comparisons were complicated by the fact that forest characteristics were different in the living and dead stands, including stand density, trunk diameter, and canopy coverage. This complication is unavoidable because severe MPB infestations kill all suitable host trees (Schmid and Mata, 1996). The trees in living stands are largely uninfested because they are different from those in the dead stands, in terms of age, species, or stand density. For example, in the current Colorado outbreak, only ponderosa pine trees with diameters <20 cm are resistant to infestation (Negrón and Popp, 2004). As in Boon (2007, 2009), the living and infested stands monitored in our study did not have identical forest characteristics.

To study the effects of tree death on snow accumulation and melt, we measured snow properties, solar radiation, and tree stand characteristics along the headwaters of the Colorado River in central Colorado. Our study differs from Boon's (2007, 2009) in three ways, and therefore provides new information about how MPB infestation impacts snow hydrology. First, the climate, topography, and forest characteristics are different at our Colorado study area. Second, we made measurements at eight pairs of living and infested forest stands, instead of a single living-infested stand pair as in Boon (2007, 2009). This allows us to quantify variability between sites and calculate statistics. Slope and aspect are similar within each site pair, yielding similar shortwave radiation at the top of the forest canopy. Third, the infested stands in our study area were in the red phase of tree death at the start of the observation period. In contrast, Boon compared grey phase stands with living stands. In the discussion, we combine our results with Boon's to develop a conceptual model of how the effects of MPB infestation on snow hydrology change throughout the sequence of forest death stages.

Most forest stands infested by MPB are composed of trees in various stages of death, as well as some living trees that are not infested (Eisenhart and Veblen, 2000; Klutsch *et al*., 2009). Similarly, nearby living stands typically include some infested trees. This complication was unavoidable in our study. In the first year of observation (2009), we identified eight site pairs with adjacent living and dead stands. The trees in the infested stands were in the red phase of the death progression. By the following year, the monitored stands provided a range of mortality comparisons because the infested stands progressed through the death stages at different rates. In addition, a significant number of trees in one of the living stands began to die. As a result, our statistical comparisons are strongest using data from the first year of observations. Our field observations were carried out in 2 years with different meteorological conditions, making comparisons between the 2 years difficult. *In lieu* of a decadal observational study on the effects of MPB on snow hydrology, we have chosen to present findings based on data collected during two field seasons. By combining our results with those from previous studies

(Boon, 2007, 2009), we are able to formulate a conceptual model that can be tested in future field efforts.

METHODS

We studied eight living/dead site pairs in the subalpine headwaters of the Colorado River (Figure 1) during the winters of 2009 and 2010. Each site pair consisted of one 3600-m^2 living lodgepole pine or mixed conifer stand and one 3600-m^2 dead lodgepole pine stand. Site pairs were initially identified and chosen based on topographic properties. Study stands range in elevation from 2680 m above sea level (asl) to 2796 m asl, and have east and west-facing slopes which range in steepness from 0·5° to 24·5° (Table I). We allowed a maximum difference between the two stands in a site pair of 15 m for elevation, 10° for slope, 45° for aspect, and 200 m for distance apart. Most pairs were much more similar than the criteria for acceptable differences stipulated. A calculation of May 1 solar radiation was made to test site pair suitability. Above-canopy shortwave radiation was projected on respective slopes for each site pair and pair-differences were <2%. This calculation does not include differences in forest characteristics. In the first winter of observations, the dead stands were in the red phase of tree death. By the second year, the dead stands were in different stages (discussed in the section on Results I: Progression of Tree Death at Study Stands).

To observe the study stands at various stages of death, we conducted a tree census at each stand measuring species dominance, tree trunk diameter at breast height (DBH), stem density, and tree mortality stage. Censuses were taken immediately following snowmelt in 2009 and 2010. The census area was demarcated by an octagon bounding line laid out with string (Figure 2). The octagon had a radius of 30 m from the central marked tree to the outer edge. Every tree within the perimeter was measured for species, DBH, mortality, and if applicable, stage of

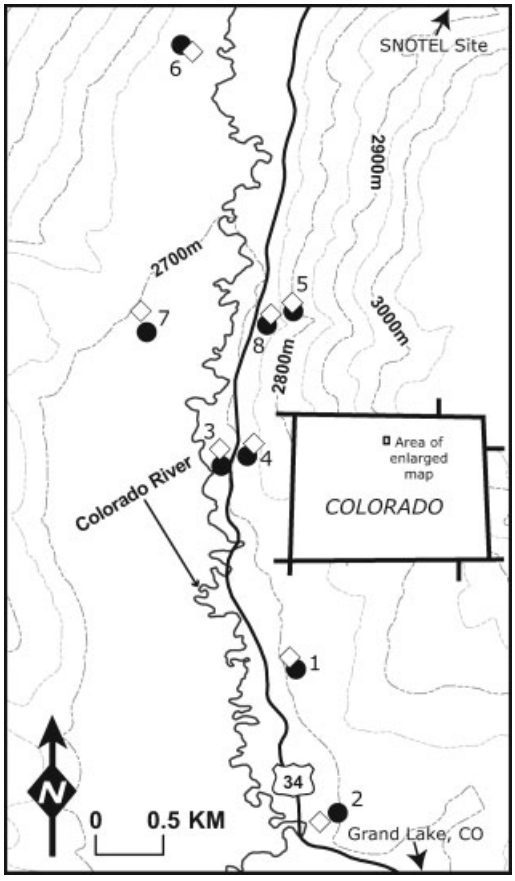

Figure 1. Site pair locations along the headwaters of the Colorado River in north central Colorado. Filled circles are living stands. Diamonds are dead stands.

Table I. Site characteristics in 2009.

Site	Initial mortality	Elevation (m)	Slope (degree)	Aspect (degree)	Forest classification	Pine composition (% stems)	Stem density (stems/ha)	Mean pine DBH (cm)	Basal area (m^2/ha)	Canopy transmission	May 1 radiation (W/m^2)
1	Living	2722	14.8	248	Mixed (E)	44.2%	1776	14·0 ± 5·3[a]	27.3	0·49 ± 0·40	5059
	Dead	2718	15.7	253	Lodgepole	73.7%	1791	18·0 ± 6·2	45.6	0·36 ± 0·28	5040
2	Living	2695	9.3	264	Mixed (S)	12.1%	2200	12·7 ± 7·9[a]	27.9	0·34 ± 0·18	4968
	Dead	2680	2.9	256	Lodgepole	87.0%	2058	17·4 ± 6·2	48.9	0·43 ± 0·29	5034
3	Living	2692	5.6	264	Mixed (L)	48.5%	3237	16·0 ± 7·1[a]	65.1	0·74 ± 0·43[a]	4953
	Dead	2690	2.5	262	Lodgepole	83.8%	1744	20·7 ± 7·8	58.7	0·18 ± 0·06	4994
4	Living	2725	14.8	285	Lodgepole	94.6%	4965	11·3 ± 4·2[a]	49.8	0·66 ± 0·45[a]	4751
	Dead	2738	17.1	267	Lodgepole	71.3%	1587	16·4 ± 5·6	33.5	0·25 ± 0·08	4826
5	Living	2789	23.7	256	Lodgepole	100%	6191	8·5 ± 4·2[a]	35.1	0·89 ± 0·30[a]	4733
	Dead	2796	24.5	257	Lodgepole	100%	1210	18·7 ± 5·6	33.2	0·64 ± 0·34	4826
6	Living	2719	4.3	88	Lodgepole	92.8%	2184	13·1 ± 6·6[a]	29.4	0·81 ± 0·42[a]	4978
	Dead	2716	2.2	71	Lodgepole	77.8%	1131	24·1 ± 10·7	51.6	0·44 ± 0·27	5000
7	Living	2697	0.5	128	Lodgepole	100%	6254	9·7 ± 4·4[a]	46.2	0·13 ± 0·01[a]	5005
	Dead	2699	1.2	122	Lodgepole	100%	786	23·6 ± 6·8	34.4	0·59 ± 0·27	5025
8	Living	2724	9.4	311	Lodgepole	87.3%	1116	22·6 ± 10·0	44.8	0·11 ± 001[a]	4701
	Dead	2725	18.4	270	Lodgepole	80.0%	786	19·5 ± 11·4	23.5	0·22 ± 0·02	4849

Mixed forests are described by the dominant species present: *L* indicates lodgepole pine (*Pinus contorta*), *E* indicates Engelmann spruce (*Picea engelmannii*), and *S* indicates subalpine fir (*Abies lasiocarpa*). May 1st radiation is the total direct radiation hitting each site on May 1st modelled from a 10 m DEM.

[a] A significant difference at $p < 0·05$.

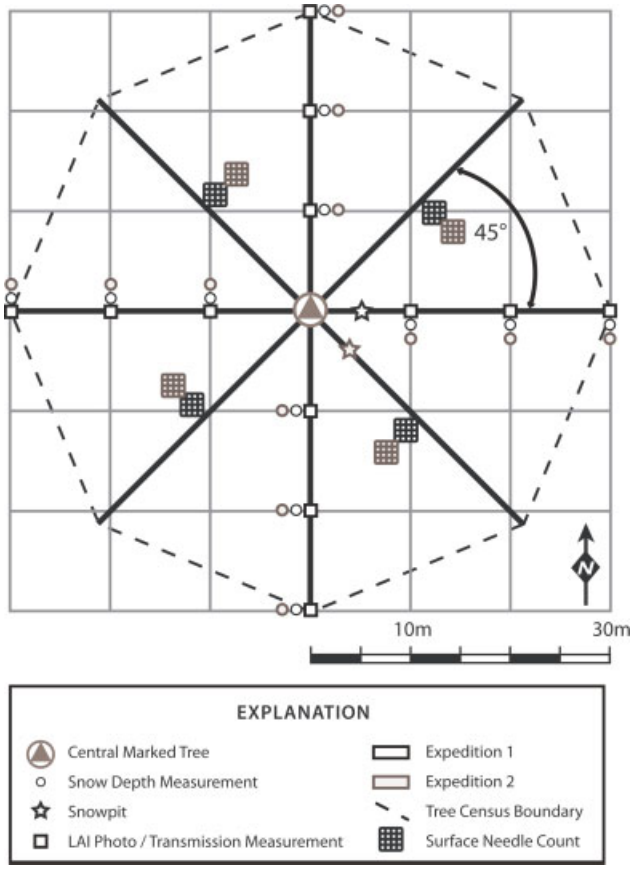

Figure 2. Study stand sampling schema. Locations of measurements taken during the first expedition of the year are marked in black. Measurement locations for the subsequent expedition are in grey.

mortality. Stand species composition, stem density, and basal area were calculated from these field data.

We divided study stands into four classifications based on the extent of tree death. Finding completely alive or dead stands was not possible given constraints on site pair proximity and topographic characteristics. Living stands were defined as stands with less than 50% tree mortality. Initially, living stands ranged from 2·5 to 48% mortality, with an average of 19·9% tree mortality. A tree's mortality was identified by the presence of red needles or total denudation. To classify dead tree stands, we used a percent grey phase relative to percent red phase ratio (G : R ratio). Red phase stands, red/grey transition stands, and grey phase stands were defined as stands with G : R ratios of less than 1, between 1 and 1·5, and greater than 1·5, respectively. Even though we use categories to describe different stages of mortality, we also analysed snow and litter properties relative to continuous measures of stand mortality.

All 16 stands were sampled between February and May of 2009 and January and May of 2010 for snowpack depth, density, and temperature. Locations of measurements within study stands can be seen in Figure 2. Monthly sampling occurred in January, February, and March; in April sampling frequency increased to bimonthly to capture the signal of ablation. Radiation was measured in June of 2009 and 2010. Snow surface litter was measured on 18 April 2010. An albedo experiment was performed on 27 April 2010.

To measure snowpack density and temperature, a snowpit was excavated at each study stand. We measured snow density using a SnowMetrics 250 cc density cutter. On each subsequent field expedition, the location selected for the snowpit was rotated 45° radially around the central marked tree to avoid anthropogenic site contamination. The snowpit was dug 5 m from the centrally marked tree. In 2009, we measured snowpack density at three depths in the snowpit to expedite measurements. Results from the three-point measurement protocol were compared with results from continuous density measurements. Differences were less than 5%. In 2010, vertically stratified measurements were made every 10 cm in the snowpit.

On each sampling trip, 12 snow depth measurements were taken at each stand. A snow probe was inserted into the snow at three locations at 10 m increments along four cardinally oriented transects originating from the centrally marked tree. On subsequent field expeditions, the snow depth measurements were taken 1 m farther from the transects to ensure undisturbed snow. SWE was then calculated using the depth-weighted snowpit density and the average plot snow depth (Boon *et al*., 2009). In early May of both years, snow cover was measured at each of the stands on three separate days. Snow cover was calculated as the ratio of snow to bare ground found along each of the four snow depth transects.

The structure of the 2009 data permitted use of nonparametric Wilcoxon signed-rank tests to identify differences in snow properties between living and dead stands (Wilcoxon, 1945). The Wilcoxon signed-rank paired test was used to analyse the 2009 data because it has fewer assumptions than comparable parametric tests. Nonetheless, a paired *t*-test yielded nearly identical results as the signed-rank test. In 2010, we monitored three mortality comparison classes (e.g. living vs grey phase). Therefore, we no longer had sufficient (∼five) site pairs in each mortality comparison class to perform a meaningful paired statistical test, either parametric or nonparametric. Therefore, we compared SWE for each site pair individually, using *t*-tests. The 12 snow depth measurements from each site were first multiplied by the single snow density value from that site prior to the statistical test. We chose to compare SWE values between site pairs, rather than simply snow depth, so that results from 2010 could be compared to those from 2009. As discussed in the results, the density data from 2009 showed that there were no significant differences in density between living and red phase stands.

iButton temperature sensors were installed in snowpits at four of the site pairs (Maxim Integrated Products Inc., 2009). At each of the stands in these site pairs, sensors were installed at depths of 12·5, 37·5, and 62·5 cm in the snowpit (roughly breaking the pit into thirds) to record continuous snowpack temperatures. The iButtons sensors were embedded 30 cm horizontally into the snowpit wall and snowpits were backfilled following sensor installation

to minimize cold wave penetration. Additional sensors were installed to measure air temperature at all site pairs.

In early June 2009 and 2010, Hukseflux LP02 pyranometers were used to directly measure the amount of solar radiation being transmitted through the canopies at all site pairs. At each stand, a mobile pyranometer was used to take 12 measurements at three evenly spaced locations along the snow depth transects originating from the centrally marked tree. Each radiation measurement was the average of 60 s at 1 s intervals. Pyranometer measurements were taken 1 m above the ground. A second pyranometer, time synchronized with the mobile one, was mounted in a nearby clearing. Canopy transmission was calculated by dividing the subcanopy radiation measurement by the clearing radiation measurement. As canopy shortwave transmission varies with solar zenith angle and diffuse skylight (Ni *et al*., 1997), measurements were made on clear and sunny days during the 2 h surrounding the solar maximum. From 2009, we have cloud-free transmission data comparing living and red phase stands. From 2010, our cloud-free transmission data compares living and grey phase stands.

Hemispherical photos were taken in November 2009 and 2010 at the same locations within each study stand as the transmission measurements. Photos were taken using a Nikon D700 camera with a Sigma EX Fisheye 8 mm lens. The camera was positioned 1 m above the ground, levelled to gravity, and oriented to true north.

In mid-April 2010, we measured snow surface litter by photographing a 1 m × 1 m PVC pipe square placed on the snow surface. At every study stand, this PVC square was placed at four locations 15 m from the centrally marked tree (Figure 2).

We performed two albedo experiments at the end of April 2010. The goal was to quantify how snow albedo changes when pine needles are added to the surface. These experiments were based on the protocol of Melloh *et al*. (2001). Lodgepole pine needles are grouped in pairs of two. We added 400 lodgepole pine needle pairs to a 0·61-m radius circle of fresh snow in increments of 50 needle pairs. Each group of 50 needle pairs weighed roughly 3 g and the 400 needle pairs had a mean length of 5·1 ± 1·1 cm. Needle pairs were placed uniformly within the circle area (Figure 3). Following each addition of more needle pairs, albedo was measured for 30 s from a height of 0·4 m with two LP02 pyranometers. The two pyranometers were mounted on a boom arm with one pointing up and one pointing down. Albedo was calculated as the ratio of incoming radiation reaching the downward-facing pyranometer. Additionally, a digital photo was taken of the circle of snow containing surface litter. This process took a total of 15 min. The experiment was first performed in a clearing and then again 10 min later in a lodgepole pine stand with a stem density of 2100 stems/ha. Before each experiment, the two pyranometers were held side-by-side in direct sunlight to ensure correct calibration. Differences were less than 1%.

In addition to adding needle pairs to the snow during each experiment, we also measured the albedo after the addition of lodgepole twigs, a 0·6-m radius black circle, and a 0·6-m radius reflective circle. The same twigs were added to both the clearing and forest sites. The twigs were added to greatly increase the percent litter cover of the snow circles. The black circle and reflective circle were measured to reveal any difference between the clearing and forest sites. The black circle was made of matte black poster board and matte black gaffer's tape. The reflective circle was made of reflective foil insulation with a bubble core. Forest albedo measurements of the black and reflective control circles were ∼15% lower on average than similar measurements taken in a clearing. Lower albedo measurements in the forest are likely due to the presence of tree trunks in the pyranometers' fields of view (i.e. the field of view extended beyond the experimental zone). The surrounding snow cover beyond the plan-view area of the experiment likely influenced the results.

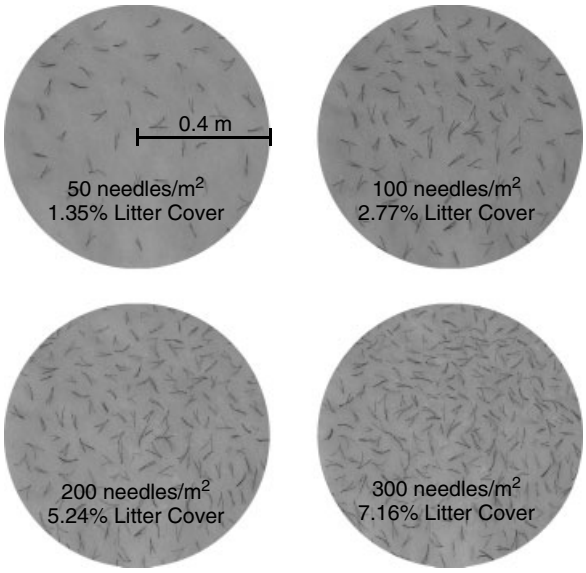

Figure 3. Example photographs of different densities of snow surface needle cover.

The digital photos taken during the snow surface litter measurements and albedo experiments were analysed to compute percent litter cover. This process consisted of converting the images to greyscale, orthorectifying the images in ESRI ArcGIS to preserve equal area between sequential photos, and finally, using the black and white threshold function in Adobe Photoshop to calculate the percentage of the image pixels that were litter and not snow. Images with high-contrast shadows were discarded.

To gauge years studied relative to long-term records, data from SNOTEL site CO05J04S (NRCS National Water and Climate Center, 2010), which is in the same valley as the study site pairs, are reported. CO05J04S is 2·5 km from the nearest study site pair (Site 5). CO05J04S has an average annual (1986–2008) air temperature of 1·2 °C with an average monthly low of −15·3 °C in January (NRCS, 2010).

Table II. Site comparison.

Site	Distance (m)	Elevation (m)	Slope (degree)	Aspect (degree)	% Difference in stem density	% Difference in DBH	% Difference in basal area	% Difference in transmission	% Difference in modelled solar
1	101	5	0.9	5	0.9	33.9	50.2	−25.7	−1.05
2	123	15	6.4	8	−6.4	37.0	54.7	26.1	1.23
3	132	1	3.2	2	−46.1	29.5	−10.3	−74.9	0.17
4	105	13	2.3	18	−68.0	45.2	−39.1	−62.7	0.86
5	72	7	0.7	2	−80.5	120	−5.6	−28.4	−0.97
6	74	4	2.1	17	−48.2	83.8	54.8	−45.4	−0.39
7	169	2	0.7	5	−87.4	143.7	−29.3	354.7	0.24
8	87	1	8.9	41	−29.6	−13.5	−62.4	102.8	0.96
Mean	108	6	3.1	12	−45.7	59.9	1.6	30.8	0.13
Maximum	169	15	8.9	41	−87.4	143.7	−62.4	354.7	1.23

Absolute values of differences between living and dead stand topographic descriptors. Percent difference (positive values are greater in the dead stand) of forest stand structure parameters and modelled incoming solar radiation between January and May 2009. All tree census data are from 2009.

RESULTS I: PROGRESSION OF TREE DEATH AT STUDY STANDS

Following each winter of snow measurements, we conducted a tree census of the study stands. Lodgepole pine is the dominant species of tree (>70% stems) at most of the study stands (Table I). Three of the living stands are composed of less than 50% lodgepole pine; these stands were classified as mixed conifer. The dominant tree species in these mixed conifer living stands are as follows: Engelmann spruce (*Picea engelmannii*) at site 1, subalpine fir (*Abies lasiocarpa*) at site 2, lodgepole pine at site 3.

Dead lodgepole stands had larger mean tree diameters than nearby living stands, but lower stem densities. The smallest trees with pitch tubes resulting from MPB attack had a DBH of 10 cm. In all but one site pair, the living stands had more stems per hectare than the dead stands against which they were compared (Table II). The biggest difference was 6254 stems/ha living to 786 stems/ha dead at site pair 7. The extreme dissimilarity of stem densities at site pair 7 makes this pair an outlier. The one site pair that did not have more stems in the living stand had a similar number of stems in both living and dead areas (1776 stems/ha living to 1791 stems/ha dead at site pair 1). Stem density and DBH did not vary greatly between 2009 and 2010.

The mortality classifications of the different study stands changed between 2009 and 2010 (Figure 4). In 2009, all eight site pair comparisons were between living stands and red phase stands. By 2010, however, only two of those living versus red phase site pairs remained. The others consisted of two living versus transitional site pairs, three living versus grey phase site pairs, and one red phase versus transitional site pair. Living stands had an average of 19·9% mortality in 2009 and 21·2% in 2010.

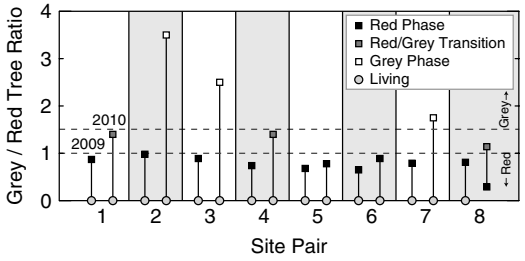

Figure 4. 2009 and 2010 mortality classifications for each site calculated by taking the ratio of grey phase dead trees to red phase dead trees (G : R ratio). Living stands have less than 50% mortality. No G : R ratio is calculated for living sites.

RESULTS II: SNOW AND RADIATION PROCESSES

From October 2008 to June 2009 (winter 2009), SNOTEL site CO05J04S recorded 50·5 cm of precipitation (NRCS, 2010). For the same time period in 2010, there was 46·7 cm of precipitation. Over the last 25 years (1984–2008), the average precipitation from October to June was 50·5 cm, with a minimum of 30·5 cm in 2002 and a maximum of 70·9 cm in 2003. The 25 year average April 1 SWE at the SNOTEL site is 35·5 cm and the standard deviation (SD) is 7 cm (NRCS, 2010). Total snow accumulation at SNOTEL site CO05J04S during the winter of 2009 was average relative to the previous 25 years. Winter 2010 had slightly below average snow accumulation. However, the 2010 snow year was anomalous in that most of the precipitation came in large late-spring storm events.

In 2009, the snowpack under living and red-phase pine stand pairs became isothermal on the same date (Figure 5). There was an initial 5-day period of isothermal snowpack beginning on 18 March. After this interval, temperatures fell back below freezing before becoming isothermal for the remainder of the melt period on 8 April. Similar amounts of snow had accumulated under living and red-phase stands on the first three sampling dates: 8 February, 8 March, and 5 April. The maximum SWE value recorded was 0·31 m at the living stand of site pair 8 on 8 March. On this date, the minimum was 0·18 m at site pairs 3 (living) and 5 (dead). Once the snowpack became isothermal for the second time, the dead pine stands had significantly lower SWE totals than their living counterparts [Wilcoxon $t(N = 8) = 18,\ p = 0{\cdot}008$].

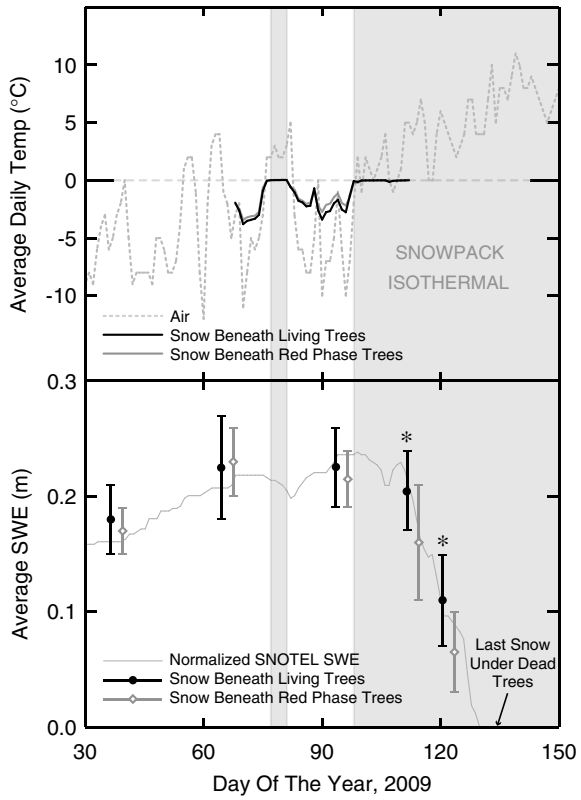

Figure 5. Temperature and SWE records for Winter 2009. Snow beneath living and red phase dead stands became isothermal on the same date. The included 2009 SNOTEL SWE record is normalized to the 25 year (1984–2008) average maximum SWE. Error bars represent 1 SD. *Indicates significant differences at $p < 0{\cdot}05$.

Once melt began, SWE was lower in the red-phase stands because snow depth was lower than in the paired live stands. No consistent differences in snowpack density were observed between site pairs during the melt interval.

The percent snow cover under red-phase pine stands was significantly lower than under living stands towards the end of the snow-covered period (Figure 6; Wilcoxon $t(N = 8) = 14$, $p = 0{\cdot}016$ on 8 May, $T(N = 8) = 10{\cdot}5$, $p = 0{\cdot}031$ on 15 May). For example, on 8 May, there was only 24% snow cover on average beneath dead stands but 68% on average under living stands. By 15 May, all snow was gone from under dead stands, while an average of 5% snow cover remained under the living stands. Snow was gone from under red-phase tree stands as much as 1 week sooner than under living stands.

Analysis of hemispherical photos shows similar percent canopy openness within living/red phase site pairs. The canopy openness values for living and red-phase stands varied from 22·4 to 30·9%. In general, stands with higher stem density had lower canopy openness. There was no significant difference in canopy openness between living and red phase stands within site pairs. The other measure of canopy transmission, direct measurement with pyranometers, showed no consistent difference between living and red phase stands. Canopies at two of the eight site pairs, site pairs 1 and 2, transmitted similar amounts of sunlight. These two site pairs were mixed conifer (living) and lodgepole (red phase). Of the remaining six site

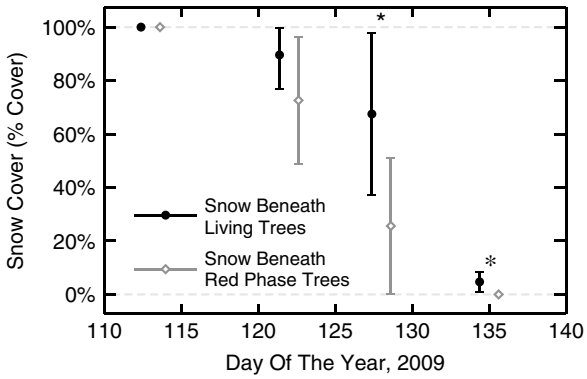

Figure 6. Percent snow cover between 20 April (DOY 110) and 20 May (DOY 140), 2009. Error bars represent 1 SD. *Indicates significant differences at $p < 0{\cdot}05$.

pairs, the living stand canopies transmitted more sunlight at four stands (t-test, $p < 0{\cdot}01$). Site pair 3, one of the four site pairs with more sunlight in the living stand, was mixed conifer (living) and lodgepole (red phase). The other three site pairs, site pairs 4–6, were made up of lodgepole (living) and lodgepole (red phase). In the two remaining site pairs, site pairs 7 and 8, the red phase stand canopies transmitted more sunlight (t-test, $p < 0{\cdot}01$). Both site pairs were composed of living and red phase lodgepole stands.

By 2010, the canopies of three stands were nearly devoid of needles. Percent canopy openness in these grey phase stands ranged from 29·2 to 38·9% and was significantly higher than the living stands within site pairs ($p < 0{\cdot}05$). Direct measurements of transmission showed significantly more solar radiation arriving in grey phase subcanopies than in their living counterparts ($p < 0{\cdot}05$). Within site pairs, grey phase canopies transmitted an average of 6·2% more solar radiation than living stands.

We now describe the time series of SWE observed in 2010 by comparison class. As discussed in the methods, the reduction in sample size due to differential progression of tree death required different statistical analyses than in 2009. Snow in red phase stands accumulated in similar amounts to the corresponding living stands. However, the snow in the red phase stands melted more rapidly [Figure 7a, $p < 0{\cdot}05$ on Day of Year (DOY) 121]. This result is consistent with our findings from 2009, which were based solely on a comparison between red phase and living stands. This significant reduction in SWE under red phase trees occurred after a considerable litter layer had appeared on the snow surface. Next, we compare accumulation and melt for the two pairs of living and red/grey transition stands. No consistent differences in accumulation or melt were observed (Figure 7b). However, there was more accumulation at one of the red/grey stands at peak SWE. Finally, more snow accumulated under all three grey phase stands than under the corresponding living stands at peak SWE (Figure 7 c, $p < 0{\cdot}05$ at peak SWE). The differences varied from 11 to 21%. The greater accumulation in dead stands was still measurable soon after ablation began (DOY 107). However, SWE was lower in the grey phase stands than

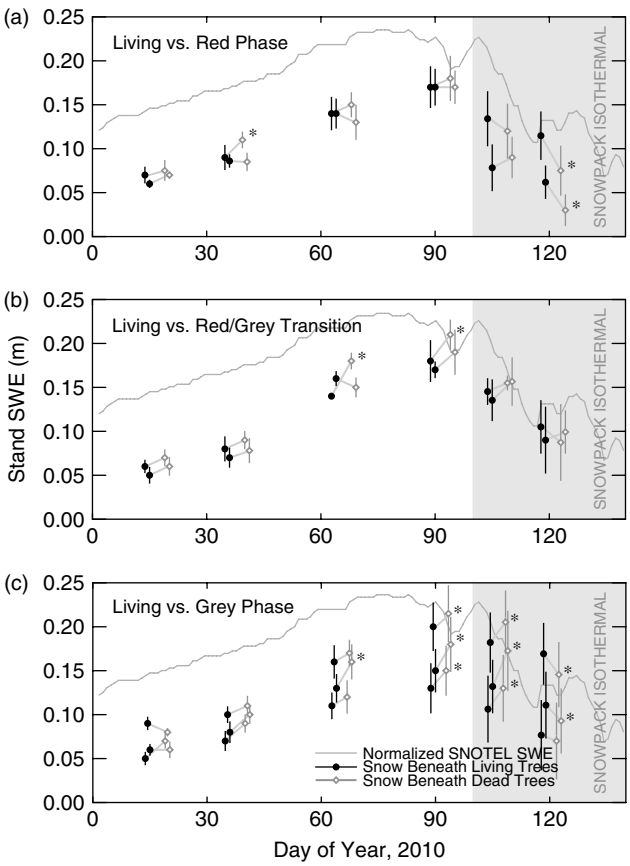

Figure 7. SWE record for Winter 2010 by mortality comparison class. *t*-tests were performed on each site pair. The included 2010 SNOTEL SWE record is normalized to the 25 year (1984–2008) average maximum SWE. Error bars represent the SD in SWE values for each stand, calculated using a single snow density measurement from each stand. *Indicates a significant difference at $p < 0{\cdot}05$.

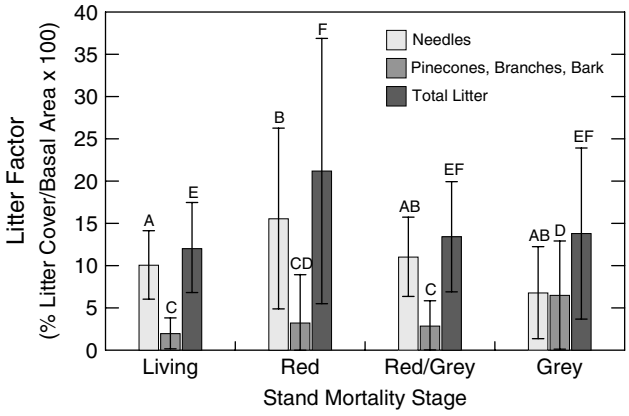

Figure 8. The amount of snow surface litter observed on 18 April 2010 at multiple sites in various stages of tree death. Snow surface litter is broken into two component parts: needles and pinecones/branches/bark. Snow surface litter is represented as litter factor, which normalizes for study stand basal area. Within each litter component classifier, dissimilar letters represent a significant difference at $p < 0{\cdot}05$. Error bars represent 1 SD.

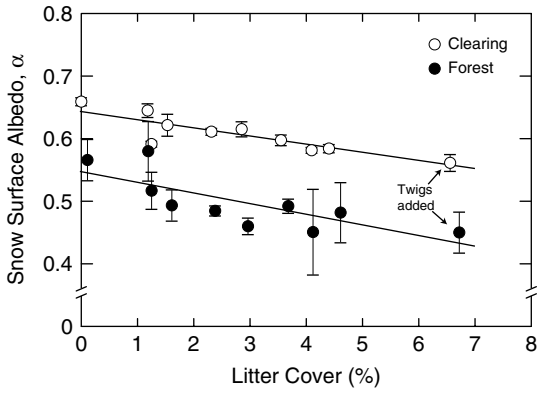

Figure 9. Variations of snow surface albedo with increasing litter cover, in a clearing and in a forest. Linear regressions of the two datasets yielded significant correlation ($p < 0{\cdot}05$): clearing (slope = $-0{\cdot}013x$, $R^2 = 0{\cdot}75$, $n = 288$) and forest (slope = $-0{\cdot}018x$, $R^2 = 0{\cdot}61$, $n = 321$). Error bars represent 1 SD.

the living stands 2 weeks later (DOY 121). This dramatic reversal in relative SWE values shows that melt was nearly twice as rapid in the grey phase stands during the middle of the ablation period.

Snow surface litter varied with tree mortality stage (Figure 8). We represent surface litter as *Litter Factor*, defined as percent litter cover divided by stand basal area, to normalize for different stand structure. Significantly more total snow surface litter existed under red phase stands than under living stands ($p < 0{\cdot}05$). When total surface litter is broken down into component parts, two additional trends are revealed. First, there are significantly more needles under red phase stands than under living stands ($p < 0{\cdot}05$). Second, there are significantly more pinecones/branches/bark under grey phase stands than under living or red/grey transitional stands ($p < 0{\cdot}05$). The highest percentages of litter cover observed were ~20% and occurred under red phase tree stands. Snow surface albedo varied with increasing litter cover in a clearing and in a forest (Figure 9). Linear regressions of the two datasets yielded significant negative correlation: clearing ($R^2 = 0{\cdot}75$, $p < 0{\cdot}01$) and forest ($R^2 = 0{\cdot}61$, $p < 0{\cdot}01$). In the discussion, we use this relationship to estimate differences in albedo between living and dead stands.

DISCUSSION

Our measurements of shortwave transmission through the canopy show no consistent differences between living and red phase stands. However, the inherent spatial variability and heterogeneous nature of canopy gaps complicate efforts to compare *in situ* measurements of canopy transmission between two different tree stands. Further complications may arise because stands do not entirely consist of trees in the same phase of mortality. Intuitively, red phase stands may transmit more radiation for two reasons. First, red phase stands appear to have predominantly downward-facing whorl orientation, which may reduce the solar shading capabilities of dead trees (Ni *et al.*, 1997). Second, as shown in the results by our surface litter measurements, red phase trees lose needles more rapidly than living trees. This needle loss should result in more pathways for sunlight to pass through red phase canopies. Although confounded by variability and spatial heterogeneity associated with canopy gaps, any differences that do exist in canopy transmission between living

and red phase stands are likely not large or would have been apparent in the measurements. In 2010, because most needles were gone from the grey phase canopies, the differences in canopy transmission between living and grey phase stands were large enough to observe. On average, grey phase stands allowed 6·2% more solar radiation through their canopies.

If the amount of solar radiation reaching the snowpack beneath living and red phase stands is similar, there must be another process driving earlier snowmelt under red phase stands. We hypothesize that the earlier snowmelt in red phase stands, compared with living stands, was caused by greater litter fall and the resulting decrease in snow surface albedo. Throughout the winter, needles and branches fall as litter into the snowpack. As melt proceeds, the litter that was distributed throughout the snowpack is concentrated at the surface lowering the snow's albedo (Pomeroy and Dion, 1996; Hardy *et al*., 1998; Melloh *et al*., 2001, 2002; Winkler *et al*., 2010). During the melt interval, there was 50% more litter at the surface in red phase stands. This is expected given that red phase trees lose all their needles in two to 3 years, compared to 9–13 years for needle turnover in healthy trees (Schoettle, 1990, 1994; Vose *et al*., 1994). Compared to living stands, the higher litter concentration in red phase stands (Figure 8) should yield lower surface albedo and greater absorption of radiation at the snow surface. We did not directly measure differences in snow surface albedo between the different mortality classes. On average, albedo should be lower by 5% in the red phase stands, using the slope of the curve in Figure 9 and observed differences in litter cover (Figure 8). At midday in May, this would yield a $\sim$30 W/m^2 increase in absorbed radiation, using the mean of our measured transmission values (0·45). The maximum observed litter cover in red phase stands was 20%, which would yield an even greater albedo change of $\sim$25%. These calculations do not consider local aspect and slope (i.e. irradiance).

Our results from the comparison of grey phase and living stands (2010 data) are largely consistent with Boon's (2009) findings. First, there is more accumulation in grey phase stands relative to comparable living stands. Second, melt is more rapid in grey phase stands. There is one notable difference. At the Colorado sites, the increase in melt rate was great enough such that SWE was lower in grey phase stands toward the end of the snow-covered period. In contrast, there was more snow in the grey phase stands throughout the melt period at the British Columbia site (Boon, 2009). There are several reasons why this difference could exist, including (1) magnitude and timing of snow accumulation during the year data were collected; (2) timing within the MPB death progression; and (3) stand characteristics and topography.

We propose the following conceptual model for MPB effects on snow accumulation and melt. It is based on results presented here and by Boon (2007, 2009). This model differs from discussions elsewhere (Boon, 2007, 2009; Potts, 1984) because it explicitly accounts for differences in processes between stands in the red and grey phases of tree death. Although we have divided the mortality stages into red and grey phases, intermediate conditions exist and are important. In addition, stand characteristics continue to change during the grey phase, as trees fall over and the understory regenerates. Even though it is simple, the model is useful for (1) guiding measurements of stand-level hydrological processes; and (2) making predictions of the effects of tree death on hydrographs.

During the red phase, trees have not yet lost significant amounts of canopy material. Therefore, there are no measurable changes in canopy snow interception or subcanopy snow accumulation at this point in the death progression. In addition, as many needles remain in the red phase canopy, any increase in transmitted shortwave radiation is negligible. Because transpiration has ceased in red phase trees, they likely retain less water than living trees. Therefore, longwave absorption and re-emission may also be smaller in the dead stands (Rouse, 1984). As a result of changes to longwave retention and emission, there may be a small advance in the date that the snowpack becomes isothermal. However, this advance was not observed here. An important difference was observed to exist during the ablation period. The rate of needle fall is several times faster in dead stands, yielding lower snow albedo and absorption of more radiation by the snowpack. The result is faster snowmelt in red phase stands. Canopy snow interception and subcanopy accumulation are not altered during the red phase of tree death. Therefore, the net input of water from snowmelt to the soil system is unchanged.

In the grey phase, more snow accumulates under dead stands than living stands because less snow is intercepted by the thinned and needle-less canopy. In addition, the thinned canopy allows for the transmission of more solar radiation to the forest floor. This leads to more rapid snowmelt in dead stands. The greater transmission of solar radiation in dead stands could also advance (1) the date the snowpack becomes isothermal and/or (2) the depletion date. Whether or not this happens depends on various hydrometeorological factors, as shown by differences between our results and Boon's (2009). The snow surface albedo is higher beneath grey phase stands, compared to living stands, because the canopy is no longer shedding needles. This albedo change would counteract the increased solar transmission and could be important in some environments (e.g. shaded slopes). The relative timing of snow depletion under grey phase and living stands depends upon the combined effects of more SWE from reduced interception versus faster melt from more transmitted radiation. Regardless of changes in melt timing, there will be more snow accumulation and less interception loss via sublimation in grey phase stands. The result is an increase in the net input of water from snowmelt to the soil system.

The magnitude of snow accumulation changes in grey phase stands, compared to living stands, was different in our study and Boon's (2009). Boon measured 74%

more SWE under grey phase stands (Boon, 2007). This observation was made during a season with unusually large SWE (159% of normal). Differences in accumulation were smaller in the following year, during which accumulation was closer to average (Boon, 2009). Our data from 2010 was measured during a winter season with below average snow accumulation. We observed additional snow accumulation in grey phase stands ranging from 11 to 21%.

The impact that increased accumulation in grey phase stands would have on streamflow is difficult to predict. Among other processes, streamflow would vary with reductions in stand evapotranspiration (Yang, 1998) and soil infiltration regimes. Additionally, it is unclear how changes in soil hydraulic conductivity associated with tree death would alter subsurface water retention, an important pre-stream hydrologic flow path in mountainous regions (Bonell, 1993). Predicting changes to impacted watershed hydrographs is outside the scope of this study.

CONCLUSIONS

We have presented a 2-year study comparing snowpack dynamics across a range of tree mortality stages. Results indicate that snow accumulation was similar under living and red phase stands, and was roughly 15% greater under grey phase stands. We observed no measurable difference in canopy shortwave transmission or percent canopy openness between living and red phase stands. Grey phase stands, however, consistently exhibited higher canopy transmission and percent canopy openness than living stands, with an average increase in transmission of 6% in dead stands. Significantly higher levels of surface litter were observed under red phase stands than under living stands. We demonstrated a strong negative linear correlation between forest litter and snow surface albedo using a simple albedo experiment. Snowpack depletion was 1 week earlier beneath red phase stands because of reduced snow surface albedo. Grey phase stands also experienced advanced ablation, likely because of increased canopy solar transmission. In the snowmelt-dominated regions of the Western United States, mountain snowpack is the largest input term in the mass balance equation that must to be solved to calculate streamflow. The observed increase in snow accumulation caused by advanced tree death would yield more water from annual snowmelt.

REFERENCES

Aukema BH, Carroll AL, Zheng Y, Zhu J, Raffa KF, Moore RD, Stahl K, Taylor SW. 2008. Movement of outbreak populations of mountain pine beetle: influences of spatiotemporal patterns and climate. *Ecography* **31**: 348–358.

Bales R, Molotch N, Painter T, Dettinger M, Rice R, Dozier J. 2006. Mountain hydrology of the western United States. *Water Resources Research* **42**: W08432. DOI:08410{DH}01029/02005WR004387.

Bernier PY. 1990. Wind speed and snow evaporation in a stand of juvenile lodgepole pine in Alberta. *Canadian Journal of Forest Research* **20**(3): 309–314.

Bethlahmy N. 1974. More streamflow after a bark beetle epidemic. *Journal of Hydrology* **23**: 185–189.

Bethlahmy N. 1975. A Colorado episode: beetle epidemic, ghost forests, more stream flow. *Northwest Science* **49**(2): 95–105.

Bonell M. 1993. Progress in the understanding of runoff generation dynamics in forests. *Journal of Hydrology* **150**: 217–275.

Boon S. 2007. Snow accumulation and ablation in a beetle-killed pine stand, northern Interior British Columbia. *BC Journal of Ecosystems and Management* **8**(3): 1–13.

Boon S, Davis R, Bladon K, Wagner M. 2009. Comparison of field techniques for measuring snow density at a point. *Streamline Watershed Management Bulletin* **12**(2): 8–12.

Boon S. 2009. Snow ablation energy balance in a dead forest stand. *Hydrological Processes* **23**: 2600–2610.

Eisenhart K, Veblen T. 2000. Dendroecological detection of spruce bark beetle outbreaks in northwestern Colorado. *Canadian Journal of Forestry Research* **30**(11): 1788–1798.

Macias Fauria M, Johnson EA. 2009. Large-scale climatic patterns and area affected by mountain pine beetle in British Columbia, Canada. *Journal of Geophysical Research* **114**: G01012.

Golding DL, Swanson RH. 1978. Snow accumulation and melt in small forest openings in Alberta. *Canadian Journal of Forestry Research* **8**: 380–388.

Hardy JP, Davis RE, Jordan R, Ni W, Woodcock CE. 1998. Snow ablation modeling in a mature aspen stand of the boreal forest. *Hydrological Processes* **12**: 1763–1778.

Hardy JP, Melloh R, Koenig G, Marks D, Winstral A, Pomeroy JW, Link T. 2004. Solar radiation transmission through conifer canopies. *Agricultural and Forest Meteorology* **126**: 257–270.

Hedstrom NR, Pomeroy JW. 1998. Measurements and modelling of snow interception in the boreal forest. *Hydrological Processes* **12**: 1611–1625.

Hibbert AR. 1965. Forest treatment affects on water yield. In *International Symposium Forest Hydrology*. Sopper WE, Lull HW (eds). Pergamon Press: New York; 527–543.

Kattelmann RC, Berg NH, Rector J. 1983. The potential for increasing streamflow from Sierra Nevada watersheds. *Water Resources Bulletin* **19**(3): 395–402.

Klutsch J, Negron J, Costello S, Rhoades C, West D, Popp J, Caissie R. 2009. Stand characteristics and downed woody debris accumulations associated with a mountain pine beetle (*Dendroctonus ponderosae* Hopkins) outbreak in Colorado. *Forest Ecology and Management* **258**(5): 641–649.

Link T, Marks D. 1999. Point simulation of seasonal snow cover dynamics beneath boreal forest canopies. *Journal of Geophysical Research* **104**(27): 27841–27857.

Link T, Marks D, Hardy JP. 2004. A deterministic method to characterize canopy radiative transfer properties. *Hydrological Processes* **18**(18): 3583.

Logan JA, Régnière J, Powell JA. 2003. Assessing the impacts of global warming on forest pest dynamics. *Frontiers in Ecology and the Environment* **1**(3): 130–137.

Love LD. 1955. The effect on stream flow of the killing of spruce and pine by the Engelmann spruce beetle. *Transactions of the American Geophysical Union* **36**(1): 113–118.

Maxim Integrated Products Inc., 2009. *Temperature logger iButton with 8 KB data-log memory data sheet*. Available at: http://datasheets.maxim-ic.com/en/ds/DS1922L-DS1922T.pdf.

Melloh R, Hardy J, Davis R, Robinson P. 2001. Spectral albedo/reflectance of littered forest snow during the melt season. *Hydrological Processes* **15**(18): 3409–3422.

Melloh R, Hardy J, Bailey R, Hall T. 2002. An efficient snow albedo model for the open and sub-canopy. *Hydrological Processes* **16**(18): 3571–3584.

Ministry of Forests and Range, 2009. *Mountain pine beetle*. Available at: http://www.for.gov.bc.ca/hfp/mountain_pine_beetle.

Molotch N, Brooks P, Burns S, Litvak M, Monson R, McConnel J, Musselman K. 2009. Ecohydrological controls on snowmelt partitioning in mixed-conifer sub-alpine forests. *Ecohydrology* **2**: 128–142.

Musselman KN, Molotch NP, Brooks PD. 2008. Effects of vegetation on snow accumulation and ablation in a mid-latitude sub-alpine forest. *Hydrological Processes* **22**: 2767–2776.

Natural Resources Conservation Service (NRCS) National Water and Climate Center. *SNOTEL data network–SNOTEL Data–all sensors*, 2010. Available at: http://www.wcc.nrcs.usda.gov/snotel/.

Negrón JF, Popp JB. 2004. Probability of ponderosa pine infestation by mountain pine beetle in the Colorado Front Range. *Forest Ecology and Management* **191**: 17–27.

Ni W, Li X, Woodcock CE, Roujean JL, Davis RE. 1997. Transmission of solar radiation in boreal conifer forests: Measurements and models. *Journal of Geophysical Research* **102**(D24): 29555–29566.

Pomeroy JW, Dion K. 1996. Winter radiation extinction and reflection in a boreal pine canopy: measurements and modeling. *Hydrological Processes* **10**: 1591–1608.

Pomeroy JW, Gray DM. 1995. *Snowcover accumulation, relocation and management*. NHRI Science Report No. 7. National Hydrology Research Institute, Environment Canada: Saskatoon, SK, Canada. 134. pp.

Pomeroy JW, Marks D, Link T, Ellis C, Hardy J, Rowlands A, Granger R. 2009. The impact of coniferous forest temperature on incoming longwave radiation to melting snow. *Hydrological Processes* **23**(17): 2513–2525.

Pomeroy JW, Schmidt RA. 1993. *The use of fractal geometry in modelling intercepted snow accumulation and sublimation*. Proceedings, 50th Annual Eastern Snow Conference. Quebec City. 1–10.

Potts DF. 1984. Hydrologic impacts of a large scale mountain pine beetle (*Dendroctonus ponderosae* Hopkins) epidemic. *Water Resources Bulletin* Paper No. 83122, **20**: 373–377.

Raynor G. 1971. Wind and temperature structure in a coniferous forest and a contiguous field. *Forest Science* **17**(3): 351–363.

Rouse WR. 1984. Microclimate at the arctic tree line. Radiation balance of tundra and forest. *Water Resource Research* **20**: 57–66.

Schmid JM, Mata SA. 1996. *Natural variability of specific forest insect populations and their associated effects in Colorado*. USDA Forest Service General Technical Report RM-GTR-275.

Schoettle AW. 1990. The interaction between leaf longevity and shoot growth and foliar biomass per shoot in *Pinus contorta* at two elevations. *Tree Physiology* **7**: 209–214.

Schoettle AW. 1994. Influence of tree size on shoot structure and physiology of *Pinus contorta* and *Pinus aristata*. *Tree Physiology* **14**: 1055–1068.

U.S. Forest Service (USFS), 2011. U.S Forest Service and Colorado State Forest Service Announce Results of Forest Health Survey. Available at: http://www.fs.usda.gov/wps/portal/fsinternet/!ut/p/c4/04_SB8K8xLLM9MSSzPy8xBz9CP0os3gjAwhwtDDw9_AI8zPyhQoY6BdkOyoCAGixyPg!/?navtype=BROWSEBYSUBJECT&cid=stelprdb5253124&navid=091000000000000&pnavid=null&ss=1102&position=News.Html&ttype=detail&pname=Region%202-%20Home/press-kits/2009/colo-aerial-survey/co-mpb-as08-8x11.pdf.

U.S. Forest Service (USFS), 2010. US Forest Service and Colorado State Forest Service announce results of Forest Health Survey. Available at: http://www.fs.fed.us/r2/news/2010/jan/nr-foresthealth-pressconf-1-22-10.pdf.

Varhola A, Coops NC, Weiler M, Moore RD. 2010. Forest canopy effects on snow accumulation and ablation: an integrative review of empirical results. *Journal of Hydrology* **319**: 219–233.

Veatch W, Brooks P, Gustafson J, Molotch N. 2009. Quantifying the effects of forest canopy cover on net snow accumulation at a continental, mid-latitude site. *Ecohydrology* **2**: 115–128.

Vose JM, Dougherty PM, Long JN, Smith FW, Gholz HL, Curran PJ. 1994. Factors influencing the amount and distribution of leaf area of pine stands. *Ecological Bulletins* **43**: 102–114.

Wilcoxon F. 1945. Individual comparisons by ranking methods. *Biometrics* **1**: 80–83.

Winkler R, Boon S, Zimonick B, Baleshta K. 2010. Assessing the effects of post-pine beetle forest litter on snow albedo. *Hydrological Processes* **24**: 803–812.

Wulder MA, White JC, Bentz B, Alvarez MF, Coops NC. 2006. Estimating the probability of mountain pine beetle red-attack damage. *Remote Sensing of Environment* **101**: 150–166.

Yang RC. 1998. Foliage and stand growth responses of semimature lodgepole pine to thinning and fertilization. *Canadian Journal of Forest Research* **28**(12): 1794–1804.